

Critical Phenomena in Nonlinear Sigma Models

Steven L. Liebling and Eric W. Hirschmann

*Theoretical and Computational Studies Group
Southampton College, Long Island University, Southampton, NY 11968*

James Isenberg

*Department of Mathematics
University of Oregon, Eugene, OR 97403*

We consider solutions to the nonlinear sigma model (wave maps) with target space S^3 and base space $3 + 1$ Minkowski space, and we find critical behavior separating singular solutions from nonsingular solutions. For families of solutions with localized spatial support a self-similar solution is found at the boundary. For other families, we find that a static solution appears to sit at the boundary. This behavior is compared to the black hole critical phenomena found by Choptuik.

98.80.-k, 11.10.Lm, 11.27.+d

I. INTRODUCTION

Nonlinear sigma models have been of considerable interest to both physicists and mathematicians for a number of years. Physicists use them to model symmetry breaking in the study of pions and other fundamental particles, and also use them to model cosmological structure formation. Mathematicians, who call them wave maps, use them as geometrically motivated, nonlinear systems of hyperbolic partial differential equations with which to study the formation and avoidance of singularities.

During the past ten years, mathematicians have proven first, that for “small data”, solutions of the Cauchy problem for wave maps avoid singularities and exist for all time (“global existence”) [1,2]. They have also been able to show that, for three or more spatial dimensions (in the base manifold), there are sets of initial data which become singular in finite time [3]. (In one spatial dimension, this cannot happen [4,5]; it is not yet clear whether singularities form in two spatial dimensions.)

These results together suggest that it could be interesting to consider one-parameter families of initial data such that for small parameter values no singularities occur, while for large values of the parameter the fields become singular. Studying the evolution of such families, one expects to see critical behavior of some sort occurring near the transition values of the parameter. The recent work by Choptuik [6] and others in which experiments such as these have been carried out with gravitational systems—collapse to a black hole for large parameter values, and dispersal for small values of the parameters—shows that very interesting phenomenology can be found at the critical, transitional, values of the parameters.

Using primarily numerical methods, we carry out such studies for spherically equivariant nonlinear sigma models with S^3 target (corresponding to the symmetry breaking $SO(4) \rightarrow SO(3)$). We find critical behavior which is

similar in some ways to that seen by Choptuik and collaborators, but very different in other ways.

We first focus on sets of initial data with localized support and finite energy. For families of such solutions, the small data global existence results hold for small values of the parameters, and the presence of critical behavior is unambiguous. We find for these families a unique, continuously self-similar solution at the threshold. This critical solution is an intermediate attractor so the critical behavior is “type II”, like that seen in critical collapse to a black hole.

Motivated by the Turok-Spergel solution [7], which is the only known explicit wave map solution which evolves from regular initial data to a singularity, we also examine sets of initial data which do not have localized support and have infinite energy. Although the small data theorem does not apply to solutions generated by such data, the “texture” studies of wave maps suggest that both nonsingular and singular solutions should occur [18,17]. Our numerical studies support this contention, and we have found that the transition is marked in some cases by the self-similar solution noted above, but in others by static solutions. While the static solutions we see at the transition are not intermediate attractors, and therefore are not critical solutions in the usual sense, our studies indicate interesting behavior which deserves further exploration.

We describe in more detail what we have learned about critical and threshold behavior for S^3 wave maps in sections III and IV. Before doing this, we briefly review in section II what wave maps are, the equations for spherically equivariant wave maps, and some of the families of initial data we use to probe the critical boundary. We describe the results of these numerical probes in section III for the families of data with localized support, and in section IV for the other families. We also note in III and IV some of the properties of the solutions found on this boundary. We make a few concluding remarks in section V.

II. SPHERICALLY EQUIVARIANT WAVE MAPS

A nonlinear sigma model, or wave map, is defined to be a map ϕ^a from a (Lorentz signature) spacetime (the “base”) into a Riemannian geometry (the “target”), with the map satisfying the differential equation

$$\partial^\mu \partial_\mu \phi^A + \Gamma_{BC}^A \partial_\mu \phi^B \partial^\mu \phi^C = 0 \quad (1)$$

where Γ_{BC}^A represents the Christoffel symbols corresponding to the metric on the target space.

In this work, we fix the base to be 3+1 Minkowski spacetime, and we fix the target to be S^3 . Furthermore, we make the spherical equivariance ansatz, which may be expressed in “hedgehog” coordinate form (for $S^3 \subset R^4$) as follows

$$\phi^a = \begin{pmatrix} \sin \chi(r, t) \sin \theta \sin m\varphi \\ \sin \chi(r, t) \sin \theta \cos m\varphi \\ \sin \chi(r, t) \cos \theta \\ \cos \chi(r, t) \end{pmatrix}, \quad (2)$$

with m a positive integer.

The only free function in (2) is the spherically symmetric function $\chi(r, t)$. It satisfies the nonlinear wave equation

$$\ddot{\chi} - \frac{1}{r^2} (r^2 \chi')' = -m(m+1) \frac{\sin(2\chi)}{2r^2}, \quad (3)$$

where prime denotes $\partial/\partial r$ and an overdot denotes $\partial/\partial t$. We enforce the regularity condition $\chi(0, t) = 0$ at the origin, and apply a standard out-going radiation boundary condition at large radius. The radial energy density corresponding to this system is

$$\rho(r, t) = \frac{r^2}{2} \left[\dot{\chi}^2 + (\chi')^2 + \frac{m(m+1)}{r^2} \sin^2 \chi \right], \quad (4)$$

with the corresponding energy function

$$E(t) = \int_r \rho(r, t) dr. \quad (5)$$

One of the features of this spherical equivariance ansatz is the possibility of nontrivial “texture charge” or “degree”. The degree of a particular wave map $\phi(r, \theta, \varphi, t_0)$ at a fixed time t_0 corresponds to the multiplicity of the covering of the target sphere S^3 (ie, the order of the third homotopy group). In terms of the hedgehog form (3), the degree depends on m , on the range of $\chi(r, t_0)$, and on certain continuity conditions at the poles of S^3 . We note that the degree is zero so long as the range of $\chi(r, t_0)$ is less than π ; if the range of $\chi(r, t_0)$ is greater than π , the degree may or may not be nonzero. The degree does not change during a smooth evolution.

If the degree of a wave map is nonzero, the energy cannot be arbitrarily small. Hence, small data arguments for global existence cannot be used. Indeed, numerical

evidence (ours and that of others) suggests that degree nonzero wave maps are inevitably singular. While this has not been proven, it leads us, in studying criticality, to focus on zero degree initial data.

To fully specify initial data, we must specify both $\chi(r, 0)$ and its time derivative at the initial time, $\dot{\chi}(r, 0)$. We then evolve this initial data with a first order formulation in which we take our fundamental fields to be $\chi(r, t)$ and $\Pi(r, t) \equiv \dot{\chi}(r, t)$. As a matter of convenience, we generally take as initial data $\Pi(r, 0) = \chi'(r, 0)$ such that the field $\chi(r, 0)$ represents an approximately in-going pulse. This choice has no affect on the critical behavior but helps to mitigate reflection from the outer boundary. Our method makes use of an iterative, second order accurate, Crank-Nicholson finite difference scheme which we have incorporated into the adaptive framework developed by Choptuik [6]. We have tested this code and shown it to converge quadratically, to conserve energy, and to be stable.

The first two families of initial data we have used to probe criticality have been chosen to have localized support and finite energy. The parameters in these families can be chosen so that the energy is very small, in which case the small data global existence results guarantee that no singularity will develop. For other parameter values, the energy is large, and the development of singularities is expected. Note that in each case, there is an amplitude A which we use to scale the data from nonsingular to singular solutions, and in addition there are two other parameters R_0 and δ which we can use to change some of the qualitative features of the family:

Gaussian Pulse Data

$$\begin{aligned} \chi(r, 0) &= Ae^{-(r-R_0)^2/\delta^2} \\ \Pi(r, 0) &= \chi'(r, 0), \end{aligned} \quad (6)$$

Logarithmic Data

$$\begin{aligned} \chi(r, 0) &= A \frac{\ln(r+R_0)}{r+\delta} \\ \Pi(r, 0) &= \chi'(r, 0) \end{aligned} \quad (7)$$

We also examine two other families of data. One of them is special in that it includes the initial data (for $\epsilon = 1$) which generates the Turok-Spergel solution [7]. This is the explicit self-similar solution which is known to evolve into a singularity in finite time. Note that the Turok-Spergel solution has nonzero degree; all others in this family (with $\epsilon < 2$) have zero degree. Note also that the energy for all of the data in this family is infinite. Therefore, we cannot use the small data global existence theorem to guarantee that solutions generated by data with ϵ small will be nonsingular. This does, however, appear to be the case (see section IV). The same is true for our fourth family of data; while there is no theoretical guarantee that both nonsingular and singular solutions are generated by data in this family, our numerical evidence supports the contention that both do occur, and so transition behavior can be studied.

Generalized Turok-Spergel Data [7]

$$\begin{aligned}\chi(r, 0) &= 2\epsilon \tan^{-1} \left(\frac{r}{\Delta} \right) \\ \Pi(r, 0) &= \frac{2\epsilon r}{\Delta^2 + r^2}.\end{aligned}\quad (8)$$

Tanh Data

$$\begin{aligned}\chi(r, 0) &= A \left[\frac{1}{2} \tanh \left(\frac{r - R_0}{\delta} \right) + \frac{1}{2} \right] \\ \Pi(r, 0) &= \chi'(r, 0).\end{aligned}\quad (9)$$

For each of the families of data listed above, our numerical studies proceed as follows: We fix a specific family by fixing a choice of R_0 and δ (or a choice of Δ) in one of the family classes listed above. With that fixed family, we run through a number of choices of A (or ϵ), from very small to large, and we evolve the solution for each choice.

In the evolved solutions, we carefully monitor the behavior of the energy density function $\rho(r, t)$ as well as that of $\chi(r, t)$; and we use these behaviors to determine which solutions become singular and which do not. Singularity formation is indicated by the unbounded growth of the derivatives χ' and $\dot{\chi}$ (and hence ρ/r^2). We find in each case that there is a critical value of A (or ϵ) which divides the initial data that evolve into a singularity from those which do not. We study very carefully the solutions at or near this critical value.

We note that while numerical results never prove that a solution is singular or not, in these studies the singular behavior appears dramatically as much of the energy density concentrates and grows without apparent bound at the origin. Note that for all of the solutions, the energy density initially flows towards the origin. In the nonsingular cases, the energy density grows at the origin, and then disperses; while in the singular cases, it continues to grow.

In the course of our studies, we have noticed another useful signal of impending singular evolution: In all cases, whenever the range of $\chi(r, t)$ exceeds π at a given time, a singularity occurs to the future. Whether or not one can indeed prove such a result, it is useful in sorting the evolutions.

III. SELF-SIMILAR SOLUTIONS AT CRITICALITY

If we consider Gaussian Pulse data for various fixed values of R_0 and δ , we find that as A approaches its critical value A^* , the corresponding solution approaches a particular self-similar solution. This critical solution is *not* the solution found by Turok and Spergel; rather it appears to be one of the sequence of self-similar solutions discovered by Aminneborg and Bergstrom [8], and subsequently Bizon [9]. These regular, self-similar solutions

obey Eq.(3) together with the scaling assumption that $\chi(r, t) = \chi(-r/t)$. The resulting equation is

$$z^2(z^2 - 1)\chi_{,zz} + 2z(z^2 - 1)\chi_{,z} + \sin(2\chi) = 0 \quad (10)$$

where the differentiation is with respect to $z \equiv -r/t$. This equation admits a countably infinite number of solutions, labeled by n , the number of times the solution crosses $\pi/2$ between $z = 0$ and $z = 1$. The Turok-Spergel solution is the $n = 0$ solution. For all n except $n = 0$, these solutions have zero texture charge. Figure 1 plots the first several solutions in this family.

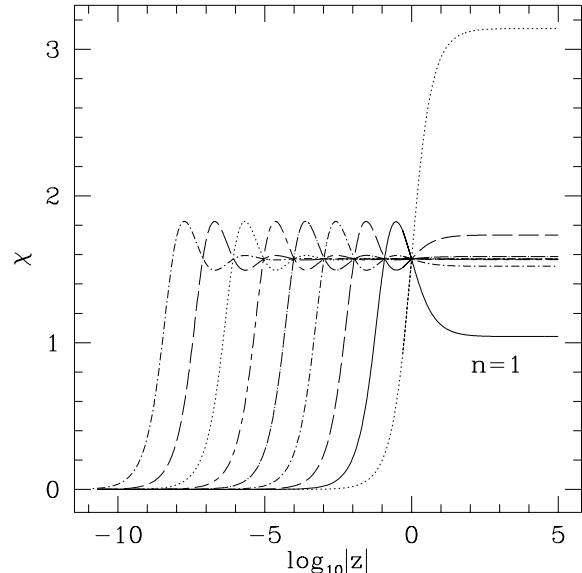


FIG. 1. These are the first nine members of the family of self-similar solutions found by Aminneborg and Bergstrom [8] as well as Bizon [9]. The $n = 0$ solution is the original Turok-Spergel solution while the $n = 1$ solution (the solid line) is the critical solution which serves as an intermediate attractor for the collapse of certain families of initial data. The label n labels the number of times χ crosses the line $\pi/2$ on the interval $(0, 1)$.

Within the range of values of r in which the near-critical solutions approach self-similarity, it is not easy to distinguish the various members of the AB sequence of solutions. In order to determine which of these solutions, which we will call AB_n , does occur on the boundary between singular and nonsingular solutions, we have examined the behavior of solutions near to several of the AB_n solutions. Specifically, on evolving members of this family, we choose a time t_0 and add a parametrized set of small amplitude Gaussian pulses to the exactly self-similar solution as initial data at t_0 for AB_n . Only for AB_1 do we find that for negative amplitude pulses, the solution is nonsingular while for positive amplitude pulses, the solution is singular. This is particularly convincing evidence that AB_1 is the critical solution, and the others are not.

In addition to the nonlinear evolution of these self-

similar solutions, we obtain further confirmation that AB_1 is the critical solution by carrying out a linear perturbation analysis for it, as well as for some of the other AB_n solutions.

Our linear perturbation analysis around this family of self-similar solutions is standard. In coordinates adapted to the self-similarity ($z \equiv -r/t$ and $\tau \equiv \ln|-t|$), the perturbed solution to leading order will be

$$\chi(r, t) = \chi_0(z) + \delta \cdot \int e^{\lambda\tau} \hat{\chi}_1(z; \lambda) d\lambda \quad (11)$$

where $\chi_0(z)$ refers to any member of the AB_n family and $\hat{\chi}_1$ is an eigenmode of the perturbation expansion associated with the eigenvalue λ . With this expansion, the eigenmodes obey the linear equation

$$z^2(z^2 - 1)\hat{\chi}_{1,zz} + 2z(z^2 - 1 - \lambda z^2)\hat{\chi}_{1,z} + (2\cos(2\chi_0) + \lambda^2 z^2 - \lambda z^2)\hat{\chi}_1 = 0. \quad (12)$$

In general, λ can be complex, but in this case it will suffice to consider λ real. As $t \rightarrow 0$, $\tau \rightarrow -\infty$, thus if $\lambda > 0$, the corresponding perturbations will decay. However, if $\lambda < 0$, the perturbations will grow and render the original self-similar solution unstable.

In order to solve the above equation it is sufficient to demand regularity at $z = 0$ and $z = 1$. On performing the integration, we find that there is a single gauge mode at $\lambda = -1$ for all members of the AB_n family. This gauge mode arises because of the freedom we have in choosing the zero of time: $t \rightarrow t + c$. In addition to this gauge mode we confirm that the Turok-Spergel solution (the $n = 0$ member of this family) has no unstable modes, the $n = 1$ member of this family has a single unstable mode, and that for all the exactly self-similar solutions we have considered with $n > 1$, there always exists more than a single unstable mode [10].

Thus this serves as further evidence that AB_1 is the critical solution. In the sense of dynamical systems, that this exactly self-similar solution has a single unstable mode indicates that it is an intermediate attractor on the boundary between the basin of attraction for singular solutions and the basin of attraction for nonsingular solutions. When such an attractor exists for critical behavior, one is said to have a ‘‘type II transition.’’

For the case of this intermediate attractor, the AB_1 solution, the eigenvalue for the single unstable mode is found to be $\lambda \approx -6.33$.

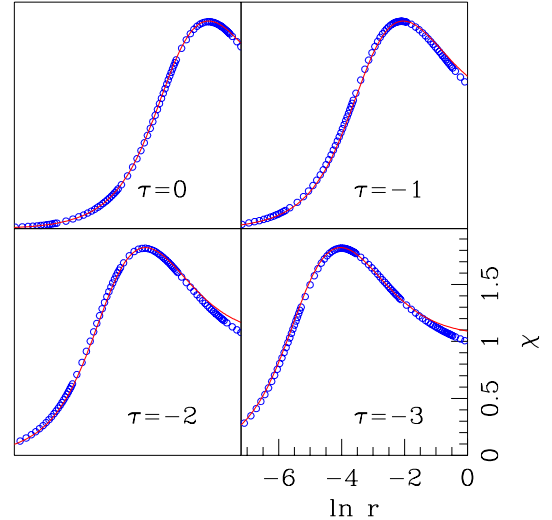


FIG. 2. Demonstration of the self-similarity of the critical solution using initial data of the form Eq.(7). Letting $\tau \equiv \ln|T^* - T|$ where T is the time of collapse, the four frames are equally spaced in ‘‘log time’’ progressing towards collapse ($\tau \rightarrow -\infty$). A near-critical solution for $\chi(r, t)$ is shown (circles) for $R_0 = 1$ and $\delta = 1$ versus $\ln r$. The $n = 1$ self-similar solution is shown (solid) with the freedom to set the collapse time used to make the two solutions coincide in the first frame only. That the solutions coincide at the other times demonstrates that the critical solution is self-similar and approaches the $n = 1$ solution.

In general, we find the same critical behavior occurring at the transition for all families of Gaussian Pulse data that we have evolved. In addition, for a number of families of Logarithmic data and even some families of the nonlocally supported Tanh data, we find AB_1 occurring at the transition as well. (Figure 2 indicates the closeness of the evolution of a near critical solution for Logarithmic data and the evolution of AB_1 .) This suggests that AB_1 is, at least in a local sense, ‘‘universal’’. Universality is a familiar occurrence in nonlinear dynamics. For example, for a damped pendulum, for all initial data except that corresponding to the stationary straight up position, the pendulum eventually ends up in the stationary straight down state. This down state is a universal attractor for the whole system.

A particularly pertinent example of similar behavior has been found in the study of black hole collapse critical behavior (for a review see [12,13]). This work has demonstrated that gravitational collapse exhibits critical solutions at the threshold of black hole formation. There, the exactly critical solution within a specific model exhibits universality as well as self-similarity (which, depending on the model investigated, can be discrete or, as here, continuous). The gravitational critical solutions are also intermediate attractors, like the AB_1 solution, in that they have a single unstable mode and sit on the

boundary between the dispersal of the collapsing matter and the formation of a black hole (*i.e.* singularity). Presumably, if we were to couple this nonlinear sigma model to gravity and evolve similar initial data, we would get black hole formation. But what is especially significant here is that even without gravity, we get singularity formation together with the universality and self-similarity seen in the gravitational context.

IV. THE ROLE OF STATIC SOLUTIONS

Consider now evolving the Generalized Turok-Spergel data for various values of ϵ . By fixing a value of Δ and considering solutions parametrized by ϵ we might expect to again get critical behavior as before. Though we do observe some sort of threshold behavior, the AB_1 self-similar solution does *not* occur at the transition. Instead, our numerical evolutions suggest that static solutions play a role in the threshold behavior.

The possibility that static solutions occur at the transition between singular and nonsingular data has led us to consider whether the static solutions are critical in this sense. To investigate this possibility, let us first consider the stability properties of the strictly static solutions.

Static solutions are studied in [14] and here we consider only those for which $\chi(0) = 0$. We could parametrize this family by $a \equiv \chi'(0)$, however, Lichtensteiger and Durrer observe that the static solutions are all related by a simple radial rescaling so we need consider only $a = 1$. We consider initial data of the form

$$\begin{aligned} \chi(r, t) &= \chi_s(r) + Ae^{-(r-R_0)^2/\delta^2} \\ \Pi(r, 0) &= \left[-\frac{r-R_0}{\delta^2} \right] Ae^{-(r-R_0)^2/\delta^2} \end{aligned} \quad (13)$$

which we proceed to evolve. The above initial data represents the static solution, $\chi_s(r)$, perturbed by an in-going Gaussian pulse. As with our non-linear perturbation of the self-similar solution, our expectation is that threshold behavior would be demonstrated if for $\chi_s(r)$ the solution becomes singular for positive amplitude perturbations ($A > 0$) but remains nonsingular for perturbations with $A < 0$. A similar test is used in [15,16] to determine whether static solutions sit on the threshold of black hole formation.

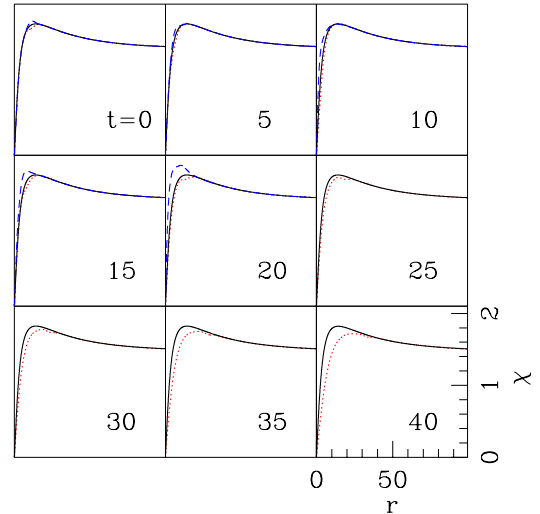


FIG. 3. Demonstration of the instability of the static solution. The static solution (solid) is perturbed with a positive amplitude Gaussian pulse (dashed) and negative amplitude (dotted). The positive perturbation collapses while the negative one disperses suggesting that the static solution sits on threshold.

An example of this experiment is shown in Fig. 3. The figure demonstrates that nonlinear perturbations of opposite sign send the static solution either to collapse or dispersal depending on the sign of the perturbation. This suggests that the static solution $\chi_s(r)$ does indeed sit on threshold.

However, if the static solution sits on threshold, one would expect that it has a single unstable mode. If so, then it should be an intermediate attractor within some basin of attraction. If it has more than one unstable mode, then we would not expect to find it via a one parameter tuning.

The mode structure for the static solution is determined by doing a linear perturbation study. Writing

$$\chi(r, t) = \chi_s(r) + \delta \cdot \int e^{-i\omega t} \tilde{\chi}_1(r; \omega) d\omega, \quad (14)$$

with $\chi_s(r)$ denoting the static solution, with $\tilde{\chi}_1(r; \omega)$ denoting the perturbation, and with ω being the eigenvalue associated with the perturbative mode $\tilde{\chi}_1$, we determine (after substituting (14) into (3)), that the perturbation modes obey

$$\tilde{\chi}_1'' = \frac{2\tilde{\chi}_1 \cos(2\chi_s)}{r^2} - \omega^2 \tilde{\chi}_1 - \frac{2}{r} \tilde{\chi}_1'. \quad (15)$$

with the regularity conditions

$$\tilde{\chi}_1(0) = 0 \quad \tilde{\chi}_1'(0) = \text{free}. \quad (16)$$

Unstable perturbation modes are signaled by $\omega^2 < 0$. We find solutions numerically, using a standard shooting

technique with the regularity condition at infinity being $\tilde{\chi}'_1(r \rightarrow \infty) = 0$. Due to the linearity of the problem, we let $\tilde{\chi}'_1(0) = 1$ and adjust ω^2 until our regularity conditions are met. We find a number of unstable ($\omega^2 < 0$) modes; it follows that the static solution does not represent an intermediate attractor.

Since the static solution is clearly not an intermediate attractor, we might not expect it to be found by tuning the Generalized Turok-Spergel initial data. For this reason, we do not view the static solution as a critical solution in the usual sense. However, it does seem to occur at the threshold, both for the Generalized T-S initial data and for a number of families of Tanh data.

Here, we might comment on some of the difficulties associated with the numerical study of solutions generated from data with infinite support:

As stated previously, fixing Δ and picking a large ϵ for the TS data, the evolution clearly demonstrates singular collapse (for $\epsilon = 1$ collapse is known). With a small value of ϵ , one might expect to observe dispersal. That is, one might expect to observe some energy density initially moving towards the origin, turning around, and then traveling outwards forever. The problem here is that numerically we can neither evolve forever nor evolve over an infinite domain. Our evolutions are limited in domain because of finite computer resources and limited in time by the adulteration of boundary effects exacerbated by the infinite nature of the initial data.

The problem of determining dispersal is less crucial for the case of Gaussian initial data and other families with localized support because we can rely on the small data global existence theorems to guarantee that the evolution is nonsingular. Here though, those theorems are not applicable because the initial data has infinite energy.

As corroborative support for our view that we are seeing nonsingular solutions, we note the work on textures in which scaling arguments are used to show that, at least for a particular class of initial data of infinite support, wave map evolutions that do not collapse can occur [18]. In fact, a number of these papers discuss the critical winding number of such textures (of infinite support) which separates dispersal from collapse (see, for example, [17]).

Our evolutions for small ϵ show what appears to be dispersal, and those for large ϵ show apparent collapse. Tuning, however, is very difficult, since (as seen in [17]), we observe solutions which at first appear to be dispersing but “turn around” and then ultimately collapse. This turn-around can occur very slowly. Hence, finding the transition is very hard.

Our evolutions therefore suggest three regimes in ϵ for the TS initial data, as well as for certain families of the Tanh data [19]. For large ϵ , the evolutions quickly collapse. For small ϵ , the evolutions suggest that the solutions do not collapse but instead disperse. For moderate ϵ , solutions appear to be dispersing but then turn around and collapse.

Given the resulting difficulty in finding a critical ϵ , one

is led to ask in what sense the static solution exhibits threshold behavior. It seems to arise for the intermediate range of ϵ as an evolving solution “turns around” from its initially outgoing, dispersive behavior and begins its collapse to a singularity. As this “turn around” point is approached, the field profiles approach that of the static solution and remain there for a certain amount of time [20]. An example of this is shown in Fig. 4. Although this behavior is certainly reminiscent of observed critical behavior, since the static solution has multiple unstable modes, it is not an intermediate attractor, and so not a critical solution in the accepted sense. However, it appears that this static solution does arise in some sense, and does play some role in wave map threshold behavior.

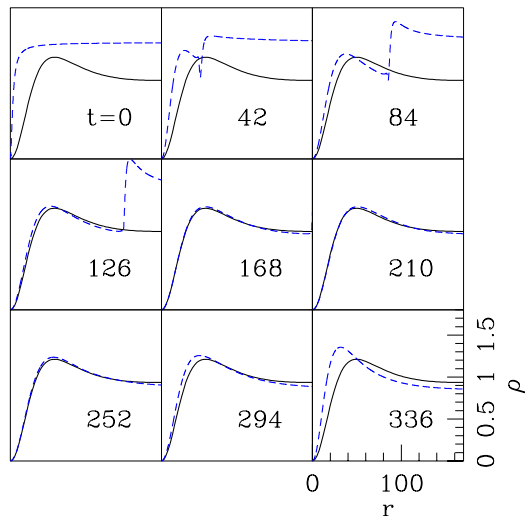


FIG. 4. Apparent approach of the tuned Turok-Spergel initial data to the static solution. Shown (dashed) is the evolution of the energy density $\rho(r, t)$ for the Turok-Spergel initial data, Eq.(8), with $\epsilon = 0.302$. The energy quickly begins to move outward to large r . However, by $t \approx 126$, the evolution has shed a large component of its energy density leaving behind an approximately static solution. Shown also is the energy density for the $a = 0.12$ static solution (solid), chosen for the best correspondence to the static part of the evolution.

The above discussion simply describes what our numerical evolutions suggest, but is clearly not definitive. Nonetheless, we conjecture that while for small ϵ data the solutions do disperse, for somewhat larger ϵ data, the solution will appear to be dispersing, but then will approach the static solution $\chi_s(r)$ (in general, for some ϵ -dependent a), and will finally collapse. Further, we conjecture that as one decreases ϵ , one will observe the solution turning around at later and later times (and larger and larger r) until for some non-zero value, ϵ^* , the solution “turns around” at infinite time and radius. Any further reduction of ϵ below ϵ^* results in dispersal.

V. CONCLUSION

Our work shows that nonlinear sigma models, or wave maps, from $3 + 1$ Minkowski spacetime into S^3 exhibit critical behavior which is similar to that seen in the study of black hole collapse for Einstein's equations with various source fields. We find that the boundary between sets of data evolving into nonsingular solutions and sets of data evolving into singular solutions includes a self-similar solution. The static solutions are found to play a role as well. The self-similar solution is an intermediate attractor, while the static solutions are not.

While this work is a first step toward understanding critical behavior in wave maps, it leaves a number of questions unanswered:

- 1) Does the critical boundary for spherically symmetric wave maps from $3+1$ Minkowski spacetime into S^3 include other solutions besides those we have seen?
- 2) How do the solutions on this boundary fit together?
- 3) What happens if one removes the spherical equivariance condition?
- 4) What happens for target spaces other than S^3 ?
- 5) What happens for base spaces other than $3+1$ Minkowski spacetime?

A base space of particular interest is $2+1$ Minkowski spacetime. For $2+1$ wave maps, it is not yet known whether in fact there are any singular solutions which evolve from regular initial data ($2+1$ is the "critical dimension" for the wave map system of partial differential equations, just as $4+1$ is the critical dimension for Yang-Mills). If such solutions exist, there would likely be critical behavior. However, one expects the nature of the critical boundary between singular and nonsingular solutions to be very different in this case. This issue is currently under study.

ACKNOWLEDGMENTS

While this work was in preparation, a preprint by Bizon [9] appeared which referred to some recent results of his and collaborators's and which has some overlap with the work described here. We are grateful for the hospitality of the ITP (supported in part by the National Science Foundation under Grant No. PHY94-07194) at the University of California, Santa Barbara at whose conference, *Classical and Quantum Physics of Strong Gravitational Fields*, this work began. Partial support for this work has come from NSF Grant PHY-9800732 at the University of Oregon. SLL and EWH are also appreciative of the financial support of Southampton College.

- [1] T. Sideris, "Global Existence of Harmonic Maps in Minkowski Space," *Comm. Pure Appl. Math.* **42**, 1-13 (1989).
- [2] Y. Choquet-Bruhat, "Global Existence for Hyperbolic Harmonic Maps," *Inst. H. Poincare Phys. Theor.* **46**, 97-111 (1987).
- [3] J. Shatah, "Weak Solutions and the Development of singularities in $SU(2)$ Sigma Models," *Comm. Pure Appl. Math.* **41**, 459-469 (1988).
- [4] C. Gu, "On the Cauchy Problem for Harmonic maps Defined on 2 Dimensional Minkowski Space," *Comm. Pure Appl. Math.* **33**, 727-737 (1980).
- [5] J. Ginibre and G. Velo, "The Global Cauchy Problem for the Nonlinear Klein-Gordon Equations," *Math. Z.* **180** 487-505 (1985).
- [6] M.W. Choptuik, "Universality and Scaling in Gravitational Collapse of a Massless Scalar Field," *Phys. Rev. Lett.* **70**, 9-12 (1993).
- [7] N. Turok and D. Spergel, "Global Texture And The Microwave Background," *Phys. Rev. Lett.* **64**, 2736 (1990).
- [8] S. Aminneborg and L. Bergstrom, "On selfsimilar global textures in an expanding universe," *Phys. Lett.* **B362**, 39 (1995) astro-ph/9511064.
- [9] P. Bizon, "Equivariant self-similar wave maps from Minkowski spacetime into 3-sphere," math-ph/9910026.
- [10] We conjecture, as do Bizon and his collaborators [9], that the n^{th} self-similar solution will have exactly n unstable modes. However, we are unaware of any proof of this and though our integrations provide evidence to this end, they do not, unfortunately, constitute proof for all n .
- [11] Because the static solution has many unstable modes, this test is only suggestive, not conclusive.
- [12] M.W. Choptuik, "The (Unstable) threshold of black hole formation," gr-qc/9803075.
- [13] C. Gundlach, "Critical phenomena in gravitational collapse," *Adv. Theor. Math. Phys.* **2**, 1 (1997) gr-qc/9712084.
- [14] L. Lichtensteiger and R. Durrer, "Are there static textures?," *Phys. Rev.* **D59**, 125007 (1999) astro-ph/9901024.
- [15] M.W. Choptuik, E.W. Hirschmann and S.L. Liebling, "Instability of an 'approximate black hole'," *Phys. Rev.* **D55**, 6014 (1997) gr-qc/9701011.
- [16] S.L. Liebling, "Critical phenomena inside global monopoles," *Phys. Rev.* **D60**, 061502 (1999) gr-qc/9904077.
- [17] A. Sornborger, "A Semi-analytical study of texture collapse," *Phys. Rev.* **D48**, 3517 (1993) astro-ph/9303005.
- [18] L. Perivolaropoulos, "Nontopological global field dynamics," *Phys. Rev.* **D46**, 1858 (1992) [hep-ph/9207256].
- [19] We do not expect, nor do we observe, initial data families of compact support finding anything other than the AB_1 self-similar solution on searching.
- [20] This time during which the evolution resembles the static solution does not appear related to tuning ϵ . Because the static solution is not an intermediate attractor, more precise tuning of epsilon does not result in a longer time.